The microstructural difference between proton-exchanged $LiNbO_3$ and $LiTaO_3$ crystals by Raman spectroscopy

1996 J. Phys.: Condens. Matter 8 2073

(http://iopscience.iop.org/0953-8984/8/12/019)

J. Phys.: Condens. Matter **8** (1996) 2073–2080. Printed in the UK

The microstructural difference between proton-exchanged $LiNbO_3$ and $LiTaO_3$ crystals by Raman spectroscopy

Xing-Long Wu†‡, Feng Yan†, Ming-Sheng Zhang†, Shu-Sheng Jiang† and Duan Feng†

† Nationl Laboratory of Solid State Microstructures and Institute of Solid State Physics, Nanjing University, Nanjing 210093, People's Republic of China

‡ Department of Chemistry, Nanjing University, Nanjing 210093, People's Republic of China

Received 23 May 1995, in final form 17 November 1995

Abstract. By means of a conventional Raman scattering technique, Raman spectra of proton-exchanged $LiNbO_3$ (PELN) and $LiTaO_3$ (PELT) crystals were examined as a function of PE time. The experimental result was that the relative intensities $I_{E(TO)}/I_{A_1(TO)}$ reach maxima and minima in PELN and PELT with about 12 and 8 h proton treatment, respectively, when y-surface cracks are visible. This phenomenon, together with the different extraordinary index changes reported previously, reflects the microstructural difference between PELN and PELT. This difference mainly arises from both the different displacements of positive ions along the optical z axis in bulk and the different proton distributions in the exchange layer due to PE.

1. Introduction

So far, most studies on proton-exchanged $LiNbO_3$ (PELN) [1–5] and $LiTaO_3$ (PELT) [6–8] have focused on layer composition, the mechanism of the exchange process and the structure of the guide layer. Little has been done about changes of the bulk phonon properties of the two protonated samples with proton-exchange (PE) time. Also, in the previous studies the exchange time was kept low and the sample subsequently annealed to remove the strains. This would be beneficial to waveguide applications. However, in our recent work [9, 10] we drew attention to the changes of bulk phonon properties with PE time by means of a conventional Raman scattering technique. The experimental results found that the E(TO) and A_1(TO) modes appear in the A_1- and E-symmetry spectra, respectively, and their intensities show a dependence on the PE time. We attributed these results to both the internal strain resulting from order–disorder distribution of protons in the samples and the changed photorefractive effect.

In this paper, we attempt to disclose the microstructural difference between PELN and PELT by examining their Raman spectra as a function of PE time. It is well known that both LT and LN are isomorphous crystals belonging to a trigonal system at room temperature. They consist of oxygen octahedra having a threefold symmetry in the plane perpendicular to the optical c axis. The oxygen octahedra with shared faces are stacked into a distorted column. In the centres of these oxygen octahedra, tantalum(niobium), lithium, and vacancies are arranged periodically. However, after PE the two protonated crystals show many different properties, in particular, in two aspects. First, the extraordinary refractive index increase $\Delta n_e = 0.02$ (at $\lambda = 632.8$ nm) [8] of the PELT waveguide is much less than that of the PELN waveguide realized under the same conditions ($\Delta n_3 = 0.12$) [11].

0953-8984/96/122073+08$19.50

Second, the PELT waveguide shows much less susceptibility to the photorefractive effect than PELN [9, 10, 12, 13] (estimated to be one to two orders of magnitude lower than for PELN). These results imply that the PE in the two ferroelectrics is somewhat different, or that the two crystals are not completely isomorphous. Thus, studies on their microstructures and phonon properties are of important theoretical and practical significance. This will be beneficial to better understanding of the characteristics of $Li_{1-x}H_xNbO_3$ and $Li_{1-x}H_xTaO_3$ bulk materials and their waveguides and further developing their applications in optical field.

2. Samples and experiments

The congruent LN and LT single crystals were grown by the Czochralski method. They were poled along the optical z axis to become single-domain crystals and then cut along the three main axes. Polishing of all faces was repeated to obtain optical-grade single crystals with sizes of $4.0 \times 2.0 \times 1.4$ and $5 \times 2 \times 2$ mm^3 ($x \times y \times z$) for LN and LT, respectively. PELN and PELT samples were prepared by immersing them in a melt of boiling nitric acid with 69 wt% at 90–100 °C for 2 h intervals, followed by air cooling to room temperature. The PELN and PELT remain transparent until the samples are treated for 12 h and 8 h, respectively, when their y-surfaces become opaque and surface cracks can be seen by using scanning electron microscopy. Raman spectra were recorded by a SPEX 1403 laser Raman spectrometer with a Datamate system to control monochromators and to carry out data processing. Right angle scattering geometries were arranged to collect the scattered light. The blue line of an argon ion laser with wavelength 488 nm was taken as an excitation source. The output power of the laser beam was set at 200 mW. The widths of both entrance and exit slits were set at 150 μm. All experiments were carried out under the same initial conditions at room temperature. In the process of every Raman spectroscopic measurement it was especially noted that the sample was laid in the proper position so that Raman excitation light can penetrate the central region of the sample, and therefore the Raman spectrum obtained can reflect information on the PE inside the sample as compared with that of a pure single crystal.

3. Experimental results

Figure 1(a)–(f) shows the Raman spectra of the pure LN substrate and PELN with the PE times of 8, 12, 14, 16 and 18 h, respectively, measured in $y(zz)x$ geometry. The spectrum (b) clearly displays the same 'leakthrough' of the E(TO) modes at 152 cm^{-1} as the spectrum (a). Figure 2 illustrates the PE time dependence of the normalized intensity for the 152 cm^{-1} E(TO) mode relative to the 254 cm^{-1} A_1(TO) mode. It can be seen from figure 2 that in the range of 4–10 h proton treatment the curve is almost flat. After 10 h treatment it rises abruptly and reaches a maximum in the sample with about 12 h treatment when y-surface cracks become visible due to the relief of internal strain [9]. After 14 h treatment the curve drops again and then rises after 16 h treatment. A similar situation can also be seen in other scattering geometries. Shown in figure 3 is the time dependence of the normalized intensity for the A_1(TO) mode at 630 cm^{-1} relative to the E(TO) mode at 580 cm^{-1}, measured in the $x(zx)y$ geometry. It is obvious from figure 3 that the curve reaches a minimum in the sample with 12 h proton treatment, corresponding to a maximum of the relative intensity I_{580}/I_{630}. This result indicates that in the sample with 12 h proton treatment the intensities of E(TO) modes reach maxima, whereas the intensities of A_1(TO) modes reach minima.

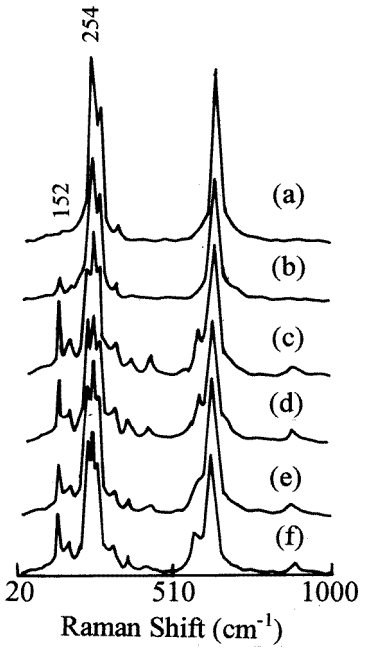

Figure 1. Raman spectra of the LN substrate and PELN with different PE times, measured in the $y(zz)x$ geometry: (a) the substrate; (b) 9 h,; (c) 12 h; (d) 14 h; (e) 16 h; (f) 18 h.

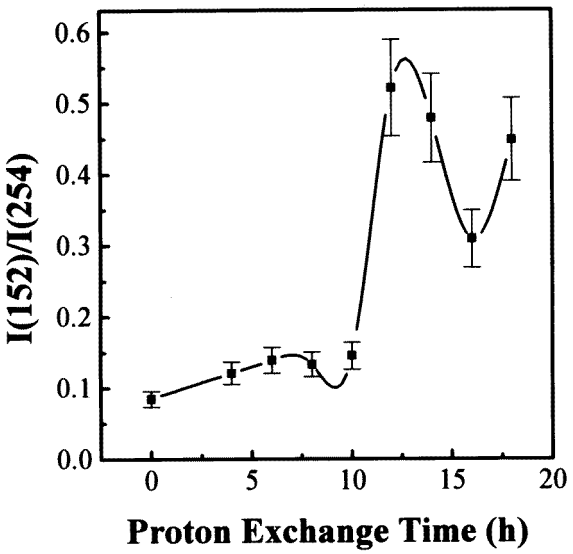

Figure 2. The PE time dependence of the normalized intensity for the E(TO) mode at 152 cm^{-1} relative to the A_1(TO) mode at 254 cm^{-1} in PELN, measured in $y(zz)x$ geometry.

Figure 4(a)–(f) shows the Raman spectra of the pure LT substrate and PELT with the PE times of 4, 6, 8, 12, and 14 h, respectively, measured in the $y(xy)x$ geometry. It can be seen from figure 4 that the intensities of E(TO) modes at 144, 208, 316, 382, and 460 cm^{-1} change

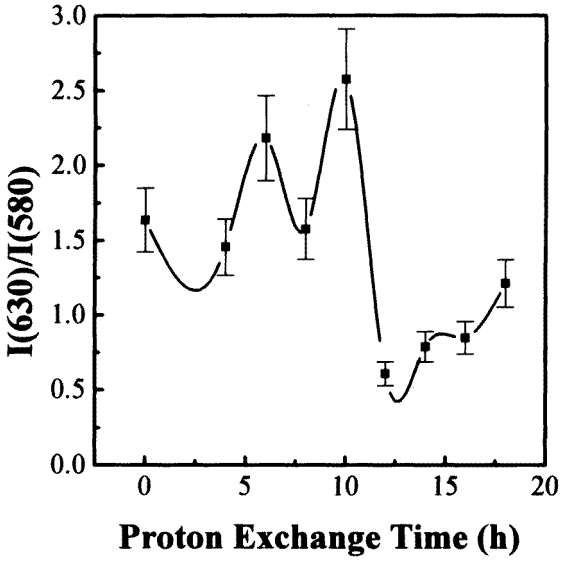

Figure 3. The PE time dependence of the normalized intensity for the A_1(TO) mode at 630 cm^{-1} relative to the E(TO) mode at 580 cm^{-1} in PELN, measured in $x(zz)z$ geometry.

with the PE time. Figure 5 displays the PE time dependence of their normalized intensities relative to the A_1(TO) mode at 596 cm^{-1}. The five curves show considerable similarity. In the sample with 8 h proton treatment, when y-surface cracks were visible, the intensities of these E(TO) modes almost reach minima and then rise abruptly. This situation is opposite to that in PELN. A similar result can also be obtained in other scattering geometries. Shown in figure 6 is the typical PE time dependence of the normalized intensity for the A_1(TO) mode at 356 cm^{-1} relative to E(TO) at 382 cm^{-1}, measured in $x(zx)z$ geometry [10]. The tendency of the curve is also opposite to that in figure 5 and is in agreement with the change of relative intensity $I_{E(TO)}/I_{A_1(TO)}$ with PE time.

From the above-obtained results, we can see an obvious difference of phonon properties between PELN and PELT. When y-surface cracks appear, the relative intensities $I_{E(TO)}/I_{A_1(TO)}$ exhibit an opposite change tendency, that is, they reach maxima and minima in PELN and PELT, respectively. This implies that the two protonated samples have an evident microstructural difference.

4. Discussion

From our previous work [9, 10], it was known that the PE process is accompanied by accumulation and relief of internal strain. According to the perturbation approach used by Barker [14], the internal strain with the four components $(s_1 - s_2)$, s_4, s_5, and s_6 can lead to an E mode becoming Raman active for (zz) incident and scattering phonon polarization. The change of the internal strain will lead to the intensity change of E(TO) modes. From the present results, it can be inferred that the internal strain reaches a maximum in the sample with about 8 and 12 h proton treatment for PELT and PELN, respectively. In addition, it is also known that the PE not only leads to a disorder of the sample surface but also causes a large lattice distortion inside the bulk [4, 15], which will lead to the change of A_1(TO) mode intensities as a result of the change of the photorefractive effect [16].

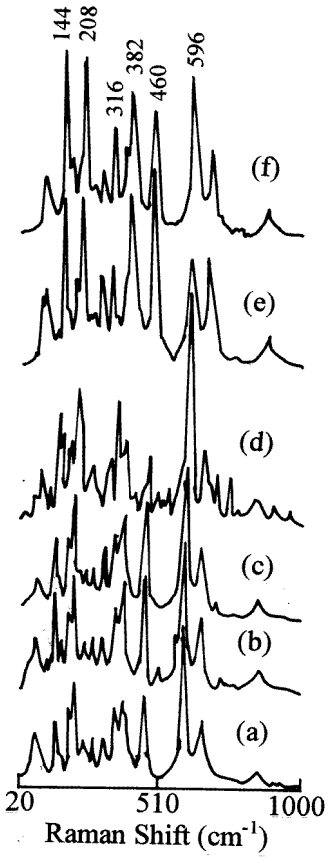

Figure 4. Raman spectra of the LT substrate and PELT with different PE times, measured in the $y(xy)x$ geometry: (a) the substrate; (b) 4 h; (c) 6 h; (d) 8 h; (e) 12 h; (f) 14 h.

Since the photorefractive effect is connected with the space charge field in the sample, the coupling of the space charge field with both the polarizing electric field accompanied by extraordinary phonons [9] and the spontaneous polarizing electric field $\boldsymbol{P}_s$ resulting from the disorder distribution of protons in the sample will lead to the change of the photorefractive effect.

The space charge field ($> 10^4$ V cm^{-1}) is far larger than the z component of the polarizing electric field [17]. Thus, the magnitude of $\boldsymbol{P}_s$ will directly affect the intensities of A_1(TO) modes. According to previous experimental results [3–5, 7], $\boldsymbol{P}_s$ mainly consists of two parts. One comes from the ion displacement resulting from a displacive mechanism of phase transition [9, 18, 19] at room temperature during the proton exchange, i.e. the sublattices of the positive lithium and niobium (or tantalum) ions moving relative to the sublattices of the oxygen anions, the displacement partially determining the direction of the spontaneous polarization $\boldsymbol{P}_s$ in the ferroelectric phase. IR spectra [2, 3, 20] of PELN and PELT showed that the protons in the protonated sample are located within the oxide planes replacing lithium ions which were in octahedral sides between those planes. Thus the replacement of lithium ions with protons leads to the distortion of bulk and surface lattices, causing displacement of positive charges (Li^+, Nb^{5+}, and Ta^{5+}) along the optical

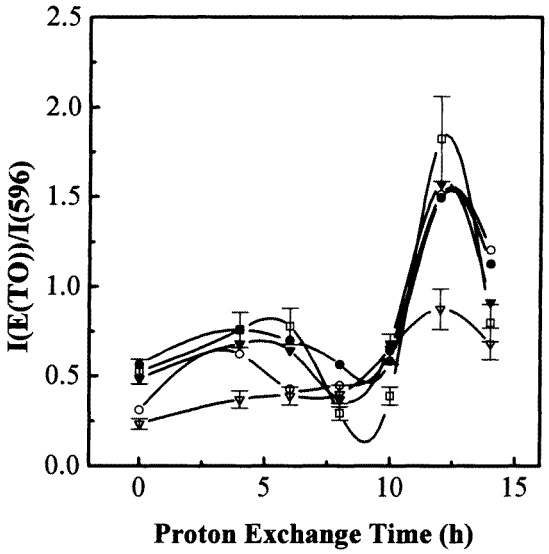

Figure 5. The PE time dependence of the normalized intensities for E(TO) modes at 14 (○), 208 (●), 316 (▽), 382 (▼), and 460 cm^{-1} (□) relative to the A_1(TO) mode at 596 cm^{-1} in PELT, measured in $y(xy)x$ geometry.

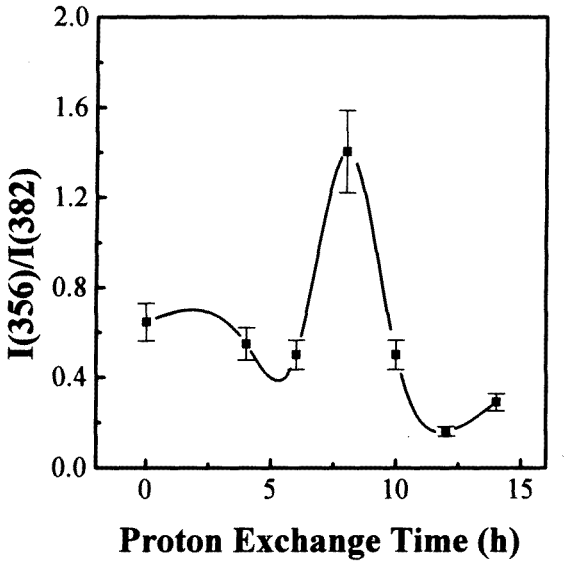

Figure 6. The PE time dependence of the normalized intensity for the A_1(TO) mode at 356 cm^{-1} relative to the E(TO) mode at 382 cm^{-1} in PELT, measured in $x(zx)x$ geometry.

z axis. RBS channelling spectra [5] from PELN showed that in a very deep disordered region near the surface of a protonated sample the niobium atoms are less displaced from their original lattice positions than tantalum atoms. IR and RBS spectra both suggest the presence of the electric field in the $-z$ direction. The other part of $\boldsymbol{P}_s$ arises from the

OH bonds formed during the proton exchange. Micro-Raman spectra [5] showed that the OH bonds in the exchange layer are polarized in the z direction, whereas IR and Raman spectra [20] showed that the OH bonds are y polarized. The two results indicate that the OH bonds may be polarized in a certain spatial direction and therefore there exists the z component of $\boldsymbol{P}_s$. The superposition between the two parts of $\boldsymbol{P}_s$ and the phonon polarizing field forms a polarizing electric field in the $-z$ direction. Both the superposed polarizing field and the space charge field have a large influence on the intensities of A_1(TO) modes. From the obtained Raman spectra, it can be seen that in the PELN and PELT samples with 12 and 8 h proton treatment, respectively, there exist the largest lattice distortions and the most disordered degree of proton distribution, and therefore we may expect a maximal $\boldsymbol{P}_s$ in the $-z$ direction. For the PELN, the result is obvious because the obtained Raman spectra show weak intensities of A_1(TO) modes as a result of the couple between the space charge field in the z direction and the strong superposed field in the $-z$ direction. However, for PELT the result is not exact because in the obtained Raman spectra the intensities of A_1(TO) modes exhibit maxima. Thus we may infer that $\boldsymbol{P}_s$ in PELN is far larger than that in PELT. The large difference of $\boldsymbol{P}_s$ may be explained from the different microstructural changes between PELT and PELN during the PE. In the process of PE, at first protons easily take the place of lithium ions in the host lattice, keeping the lattice distortion less and the disordered degree lower. When the proton concentration reaches a certain intensity, not all protons will substitute directly for lithium ions but some of them may be in interstitial positions. The substitutional protons do not occupy exactly the ferroelectric positions of lithium ions but are situated within the oxide plane. The replacement of a lithium ion by a proton leads to a displacement of a positive charge. The displacement is intimately related to the electronegativity, the coordination number, and the ionic radii of this ion. Since the tantalum ion has a smaller ionic radius than the niobium ion, the tantalum ion has less displacement in the z direction than the niobium ion due to lattice distortion, which leads to the weak $\boldsymbol{P}_s$. Thus the oxygen octahedra centred with tantalum ions are more stable than those with niobium ions and the PELT has less lattice distortion than the PELN.

According to the above analysis, we may explain different changes of the extraordinary refractive indice between PELT and PELN. The proton exchange results in a displacement of positive charge ions along the optical z axis. This might be expected to increase the polarizability of the oxygens more distant from the positive ion, while decreasing the polarizability of the closer oxygens. Since in PELT the positive ion has less displacement from the original ferroelectric position than that in PELN, the PELT shows less change of the extraordinary refractive index than the PELN. The difference of Δn_e is directly related to the magnitude of positive charge displacement.

5. Conclusion

In this paper we have examined the Raman spectra of protonated LN and LT as a function of PE time. It was found that in the PELT and PELT samples with 8 and 12 h proton treatment, the relative intensities $I_{E(TO)}/I_{A_1(TO)}$ show minima and maxima, respectively. The phenomenon consistent with the extraordinary refractive index change really reflects the microstructural difference between PELT and PELN. The tantalum ion has less displacement from the original ferroelectric position than the niobium ion, leading to more stable structure of oxygen octahedra and meantime displaying less change of the extraordinary refractive index.

Acknowledgment

This work was supported by the Ke-li fellowship.

References

[1] Jackel J L, Rice C E and Veselka J J 1982 *Appl. Phys. Lett.* **41** 607
[2] Canali C, Carnera A, Mea G D, Mazzoldi P, Al Shukri S M, Nutt A C G and De La Rue R M 1986 *J. Appl. Phys.* **59** 2643
[3] Rice C E 1986 *J. Solid State Chem.* **64** 188
[4] Savatinova I, Tonchev S, Popov E, Liarokapis E and Raptis C 1992 *J. Phys. D: Appl. Phys.* **25** 106
[5] Paz-pujalt G R, Tuschel D D, Braunstein G, Blanton T, Lee S T and Salter L M 1994 *J. Appl. Phys.* **76** 3981
[6] Findakly T, Suchoski P and Leonberger F 1988 *Opt. Lett.* **13** 797
[7] Mattheus P J, Mickelson A R and Novak S W 1992 *J. Appl. Phys.* **72** 2562
[8] Savatinova I, Tonchev S, Kuneva M and Liarokapis E 1994 *Appl. Phys.* A **58** 481
[9] Wu X L, Zhang M S, Yan F and Feng D 1995 *J. Appl. Phys.* **78** 1953
[10] Wu X L, Zhang M S and Feng D *Phys. Status Solidi* at press
[11] Ziling C, Pokrovskii L, Terpugov N, Savatinava I, Kuneva M, Tonchev S, Armenise M N and Passaro V M N 1993 *J. Appl. Phys.* **73** 3125
[12] Tangonan G, Barnoski M, Lotspeich J and Lee A 1977 *Appl. Phys. Lett.* **30** 238
[13] Tsuya H 1975 *J. Appl. Phys.* **46** 4323
[14] Barker A S Jr 1963 *Phys. Rev.* **132** 1475
[15] Savatinova I, Tonchev S and Kuneva M 1993 *Appl. Phys.* A **56** 81
[16] Chen F S 1969 *J. Appl. Phys.* **40** 3389
[17] Schein L B and Cressman P J 1977 *Appl. Phys. Lett.* **48** 4844
[18] Zhang M S and Scott J F 1986 *Phys. Rev.* B **34** 1880
[19] Okamoto Y, Wang P C and Scott J F 1985 *Phys. Rev.* B **32** 6787
[20] Kapphan S and Breitkopf A 1992 *Phys. Status Solidi* a **133** 159